

ITRI

NASA CR 70780

N66-20053

FACILITY FORM 802

(ACCESSION NUMBER)  
69  
(PAGE)  
CL 70780  
(NASA CR OR TMX OR AD NUMBER)

(CR#)  
1  
(CODE)  
26  
(CATEGORY)

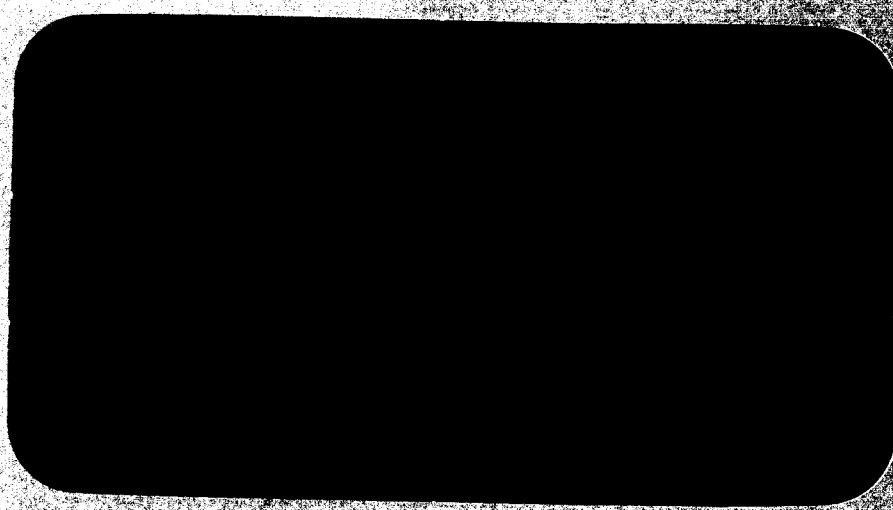
GPO PRICE \$ \_\_\_\_\_

CFSTI PRICE(S) \$ \_\_\_\_\_

Hard copy (HC) 300

Microfiche (MF) 75

# 653 July 65



Report No. IITRI-U6004-21  
(Summary Technical Report)

STABLE WHITE COATINGS

Jet Propulsion Laboratory

IIT RESEARCH INSTITUTE

Report No. IITRI-U6004-21  
(Summary Technical Report)

STABLE WHITE COATINGS

July 3, 1964, through December 1, 1965

Contract No. 950746  
IITRI Project U6004

Prepared by

J. E. Gilligan

of

IIT RESEARCH INSTITUTE  
Technology Center  
Chicago, Illinois 60616

for

Jet Propulsion Laboratory  
California Institute of Technology  
4800 Oak Grove Drive  
Pasadena, California

Copy No. 96

February 7, 1966

IIT RESEARCH INSTITUTE

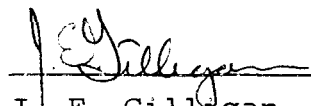
## FOREWORD

This is Report No. IITRI-U6004-21 (Summary Technical Report) of IITRI Project U6004, Contract No. 950746 (subcontract with the Jet Propulsion Laboratory of the California Institute of Technology under NASA Contract NAS7-100), entitled "Stable White Coatings." It covers the period July 3, 1964, through December 1, 1965, and has been prepared for Mr. William M. Hall, JPL Cognizant Engineer.

Major contributors to this program were J. E. Gilligan (Project Leader), Noel D. Bennett (reflectance measurements and equipment operation), William F. Logan (sample preparations), James A. Hodges (ESR spectra), Irene Corvin (x-ray diffraction), Dr. E. L. Grove (chemical and spectroscopic analyses), and G. A. Zerlaut (general consultation). Dr. Theodore H. Meltzer, Manager, Polymer Chemistry, administered the program.

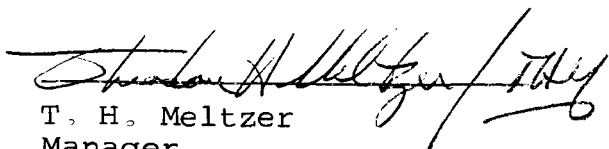
Respectfully submitted,

IIT RESEARCH INSTITUTE



J. E. Gilligan  
Research Engineer  
Polymer Research

Approved by:



T. H. Meltzer  
Manager  
Polymer Research

JEG/jab

IIT RESEARCH INSTITUTE

ABSTRACT

20053

STABLE WHITE COATINGS

This report presents the results of a program to study the induced optical properties and the photoreactions of zinc oxide. An analysis of the findings of an extensive literature search formed the basis of the experimental plan adopted in this program.

Luminescence studies, chemical analyses, x-ray diffraction studies, reflectance measurements, and numerous mechanical and thermal treatments were carried out. For the most part the results compare well with the more commonly accepted results reported in the literature. It was conclusively established that ultraviolet-induced absorption in the infrared spectrum can be completely extinguished in a matter of seconds simply by increasing the environmental pressure to atmospheric. This finding will drastically alter many current concepts of space materials testing. The infrared bleaching effect in zinc oxide, whether it is limited to zinc oxide or not, will discourage automatic acceptance of routine pre- and post-test ultraviolet irradiation data at least until competent testing establishes which materials need in situ testing and which do not.

*Author*

IIT RESEARCH INSTITUTE

## TABLE OF CONTENTS

|  | Page |
|--|------|
| Abstract   | iii  |
| I. Introduction                                    | 1    |
| II. Zinc Oxide Preparation and Characterization    | 2    |
| A. Preparation                                     | 2    |
| B. Measurement Techniques                          | 4    |
| C. Chemical Analyses                               | 5    |
| D. X-Ray Diffraction                               | 9    |
| III. Literature Survey                             | 12   |
| IV. Experiments and Results                        | 22   |
| A. Mechanical/Thermal Treatments                   | 22   |
| B. Luminescence                                    | 29   |
| C. Proton Irradiation                              | 36   |
| D. Induced Infrared Absorption                     | 37   |
| V. Summary and Conclusions (The Photolysis Scheme) | 45   |
| References   | 52   |



## LIST OF TABLES

| TABLE |   | Page |
|-------|---|------|
| 1     | Flame Spectrophotometric Analysis of Lithium-Doped SP500 Zinc Oxide         | 6    |
| 2     | Qualitative Spectrographic Analysis of Various Zinc Oxide Samples           | 7    |
| 3     | Spectrographic Analysis of Zinc Oxide Crystals                              | 8    |
| 4     | Lattice Parameters of Zinc Oxide  | 11   |
| 5     | Mechanically/Thermally Treated Zinc Oxide                                   | 24   |
| 6     | Slit Control and Spectral Resolution of the Beckman DK-2A Spectrophotometer | 27   |
| 7     | Luminescence of Various Zinc Oxide Samples                                  | 30   |

## LIST OF FIGURES

| FIGURE |   | Page |
|--------|---|------|
| 1      | Debye-Scherrer Powder Photographs of Untreated and Ball-Milled Zinc Oxide | 10   |
| 2      | Generalized Mechanical/Thermal Damage Spectra                             | 25   |
| 3      | Luminescence Spectra of Various Zinc Oxide Samples at 2750-Å Excitation   | 31   |
| 4      | Ultraviolet in Situ Reflectance Apparatus                                 | 38   |
| 5      | Reflectance Spectra of Various Zinc Oxide Samples                         | 40   |
| 6      | Electronic Band Structure of Zinc Oxide                                   | 47   |
| 7      | Ultraviolet-Induced Depletion of Band Curvature                           | 48   |



## STABLE WHITE COATINGS

### I. INTRODUCTION

Despite many searching investigations, the optical and the electrical behavior of zinc oxide are very difficult to understand. An enormity of facts and observations concerning the behavior of zinc oxide in various states and forms under different environments can easily be cataloged; in contrast, comparatively few remarks can be made in explanation of these facts and observations.

The objective of the present investigation was to correlate the static and dynamic optical properties of zinc oxide as measured in our laboratory with those reported in the literature. There were two principal problems. One is that ultraviolet photolysis has not been extensively studied in terms of effects on optical properties. The other is that very important differences and discrepancies occur in the results of apparently identical experiments. We cannot with certainty state which data are correct or otherwise, nor was this our intent. Our approach was to study the literature and to try to duplicate those experiments that seemed not only relevant but important in explaining the optical photolysis of zinc oxide.

The investigations were principally in the realm of applied research. We sought to establish in fundamental terms the facts that require explanations and their explanation.

IIT RESEARCH INSTITUTE

Thus, we asked what happens to the optical properties of zinc oxide when irradiated or mechanically/thermally treated, what is the nature of the defects thus created, and which defects are responsible for the optical absorption induced.

The principal induced optical effects in zinc oxide are only two. One effect is induced by ultraviolet irradiation and appears very rapidly, in less than 0.1 equivalent solar-hour. The second effect is induced in a number of ways, e.g., mechanical (abrasion and milling) and thermal treatments. The first effect can be observed only when zinc oxide is in a high-vacuum environment; it appears as an absorption that increases with increasing wavelength. The second effect results from an induced absorption band with a classical Lorentzian shape, a very narrow band centered at approximately 3850 Å.

We have included as much background data as is necessary to understand the experimental plan and its results.

## II. ZINC OXIDE PREPARATION AND CHARACTERIZATION

### A. Preparation

To avoid characterization and reproducibility problems, only one zinc oxide was studied: New Jersey Zinc SP500. This material is commercially available and was not treated prior to any of the special treatments discussed. All the samples were powders and were prepared in one of two forms, either as a pressed compact or as a hot sprayed dust.

The compacts were formed by hand-pressing the material into a 1-in.-diameter 0.025-in.-deep recess in a brass mold. Laboratory glass slides were used to smooth the powder surface and to compact the powder just enough to form a cohesive, opaque layer. This compaction operation did not result in any detectable mechanical damage. In most cases the compaction was sufficient to maintain the integrity of the compact even when it was turned over.

The dust films consisted of a thin but opaque layer of material deposited on a suitable substrate, usually aluminum. These films adhered quite well but required delicate handling to prevent their being rubbed off. They gave high and reproducible reflectance spectra, comparable to those obtained with the optically thick compacts. Their thickness was not measured.

The hot spraying process starts with the preparation of a water slurry of the material and results in a dry dust film applied to a hot substrate. Several variations of this technique were used to obtain opaque coatings on various substrates without introducing further damage to or treatment of the deposited material. The "trick" in this technique hinges upon the nearly immediate evaporation of the water vehicle during the spraying process. Most often evaporation is encouraged by maintaining the substrate at moderately high temperature. In all cases results were quite good and, more important, very uniform. Reproducibility was not a problem.

IIT RESEARCH INSTITUTE

## B. Measurement Techniques

The spectral reflectance data were obtained on a Beckman DK-2A spectroreflectometer through ratio measurements in the optical density mode. By this technique the log of the ratio of the spectral reflectance of a standard ( $R_0$ ) to the spectral reflectance of the sample ( $R_s$ ) is obtained. This method has the advantage that all spurious or characteristic effects are either determined or cancelled. Accordingly, only changes in spectral reflectance appear. In interpreting these data, we assume that the optical properties of the window materials do not deteriorate. Hence, the ratio,  $R_s/R_0$ , sensitively indicates the change in reflectance occurring in one beam path of the spectrophotometer versus that occurring in the other. In the optical density (OD) mode, the measured quantity  $\log_{10} (R_0/R_s)$  gives a reasonably sensitive indication of changes in  $R_s$ .

For example, a decrease in reflectance from 0.95 to 0.85 would register as a 0.05 change in OD. More important, however, is that OD reflects the induced change in the absorption constant,  $K$ , as expressed in the relation:

$$\Delta R(E) = \exp - \{aK(E)\}$$

where

$E$  is photon energy

$a$  is an energy-dependent parameter that accounts for thickness, scattering, and other effects.

Hence, reflectance OD has a more fundamental meaning than absolute reflectance. Its behavior can be used to study and characterize the nature of any induced optical damage.

The measurement procedure was as follows.

(1) After the spectrophotometer was set at zero, the 100% value was set by placing identical untreated SP500 compacts in both the reference and the sample ports. Scans from 0.7 to 0.35  $\mu$  indicated minor ( $<0.02$ ) variations from unity in ratios of identical, untreated samples.

(2) The SP500 in the sample port was then replaced with the treated sample and scans of  $R_s/R_0$  and  $\log_{10} (R_0/R_s)$  from 2.7 to 0.35  $\mu$  were made.

(3)  $R_s/R_0$  and  $\log_{10} (R_0/R_s)$  scans were rerun after  $R_s/R_0$  was set equal to unity at 0.7  $\mu$ . With this normalization process  $\log R_0$  is zero, and  $\log R_s$  thus describes the induced absorption.

(4) The wavelength drive was manually operated to determine the exact wavelength at which  $R_s/R_0$  was a minimum and its value at this wavelength. The OD scan was then made, followed by a similar procedure for determining positions and values of the maxima.

### C. Chemical Analyses

Two separate analyses were made of several zinc oxide materials. The data in Table 1 were obtained by using calibrated standards in a flame spectrophotometric technique,

which gives results accurate to 0.1 ppm. Table 2 gives the results of an analysis by emission spectrography. A scan for the presence of more than 40 elements was made by looking for RU (most sensitive) lines. On this basis, elements other than those listed may be present, but to an extent much less than 1 ppm. Compared to SP500, the purity of commercial zinc oxide leaves much to be desired. For comparison, the spectrographic impurity data of zinc oxide crystals grown by Minnesota Mining and Manufacturing Company are presented in Table 3 (ref. 1).

Table 1

FLAME SPECTROPHOTOMETRIC ANALYSIS OF LITHIUM-DOPED ZINC OXIDE

| <u>Sample</u>                           | <u>Li Detected, ppm</u> |
|---|-------------------------|
| SP500                                   | -                       |
| New Jersey Zinc<br>undoped control      | -                       |
| New Jersey Zinc<br>Li-doped 0.01 mole % | 9.2                     |
| New Jersey Zinc<br>Li-doped 0.1 mole %  | 75                      |

Table 2

## QUALITATIVE SPECTROGRAPHIC ANALYSIS OF VARIOUS ZINC OXIDE SAMPLES

| Sample                                     | Analysis <sup>a</sup> |    |    |    |    |    |    |    |
|--|-----------------------|----|----|----|----|----|----|----|
|  | Al                    | Ca | Cr | Cu | Fe | Li | Mg | Si |
| SP500                                      | -                     | W  | -  | VW | -  | -  | FT | FT |
| New Jersey Zinc<br>undoped                 | -                     | W  | -  | VW | -  | W  | T  | FT |
| New Jersey Zinc<br>Li-doped<br>0.01 mole % | -                     | VW | -  | VW | -  | W  | FT | FT |
| Baker and Adamson<br>CP 2451               | T                     | M  | T  | W  | T  | -  | W  | W  |

<sup>a</sup>FT, faint trace, 5 ppm; T, trace, 1-10 ppm; VW, very weak, 5-15 ppm; W, weak, 10-100 ppm; M, moderate, 100 ppm.



Table 3  
SPECTROGRAPHIC ANALYSIS OF ZINC OXIDE CRYSTALS

| <u>Element</u> | <u>Ppm</u> |
|----------------|------------|
| As             | -          |
| Te             | -          |
| B*             | 10         |
| Pb             | -          |
| Mg             | 5          |
| Si             | -          |
| Sb             | -          |
| Ni             | 1          |
| Fe             | -          |
| Cr             | -          |
| In             | -          |
| Bi             | 5          |
| Al             | -          |
| Be             | -          |
| Sn             | 1          |
| Mo             | 0          |
| V              | 1          |
| Ti             | -          |
| Cu             | 3          |
| Mn             | -          |
| Ag             | 1          |
| Co             | -          |
| Ca             | 1          |
| Sr             | -          |
| Ba             | -          |
| Cd             | -          |
| Cl             | Not tested |
| K              | 1          |
| Li             | 1          |
| Na             | 1          |
| Ge             | 1          |

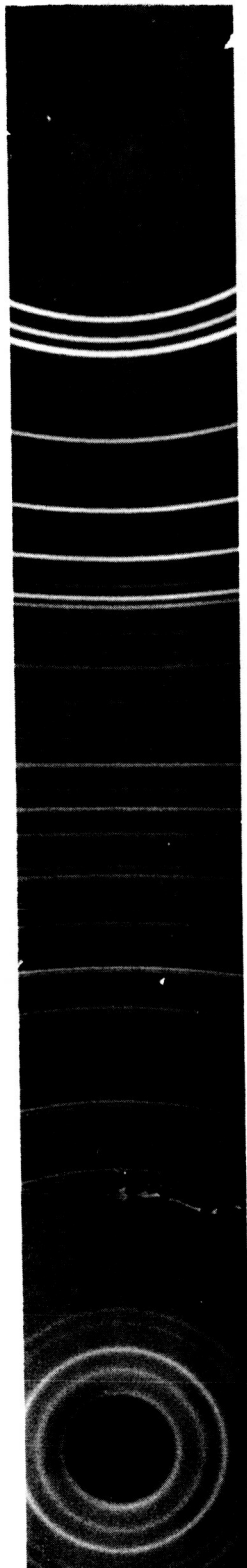
\*  
Subjected to contamination on grinding.

#### D. X-Ray Diffraction

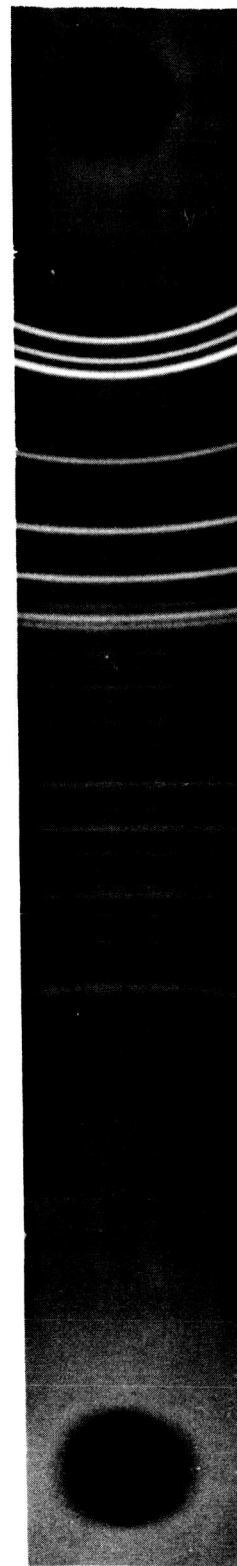
Untreated SP500 zinc oxide and SP500 ball-milled for 48 hr with corundum balls were examined by x-ray diffraction to detect any differences that might be caused by ball milling. The control sample was white, and the ball-milled sample was yellowish tan.

Each sample was mounted in a 0.3-mm ID pyrex capillary tube, and Debye-Scherrer powder photographs were taken by using copper  $K\alpha$  radiation at 40 kV and 18 ma. The untreated specimen (Figure 1a) consisted of sharp lines throughout the whole film, with the copper  $K\alpha_1\alpha_2$  doublet well resolved in the back reflection region. This pattern indicates an average crystallite size of approximately  $10^{-4}$  cm, or  $1\ \mu$ . The ball-milled specimen (Figure 1b) had somewhat less sharp lines in the forward reflection of the film. However, as the Bragg angle increased, the broadness of the lines increased considerably, the copper  $K\alpha_1\alpha_2$  components were no longer resolved, and the intensity of the lines decreased markedly as compared to the corresponding lines in the control sample. The broadness indicates an approximate crystallite size of  $0.1\ \mu$  or less, if it is assumed that the broadening can be ascribed to small crystallite size only.

However, line broadening is a complex phenomenon, and small crystallite size is only one possible contributing factor. Various stress effects are also known to broaden diffraction lines markedly. Because of the severe cold work sustained by



1a



1b

Figure 1

DEBYE-SCHERRER POWDER PHOTOGRAPHS  
OF UNTREATED AND BALL-MILLED ZINC OXIDE

the specimen, various kinds of stresses are undoubtedly present. These include microstresses, which are variations in stress in different regions of grains or subgrains, so that interplanar spacings may vary from region to region; bending stresses in the individual crystallites; and stacking fault disorders.

Many attempts to separate line broadening effects have been reported in the literature. Crystallite size broadening has been found to be proportional to  $1/\cos \theta$ , and the stress effects are proportional to  $\tan \theta$ . A systematic x-ray diffractometric investigation in which line contours are recorded and the broadening determined quantitatively as a function of the degree of mechanical damage might prove informative. Crystallite size and stress effects are often superimposed, so that it is difficult to decide how much of each contributes to the line broadening.

Lattice parameter calculations (Table 4) for both specimens showed essentially no difference.

Table 4  
LATTICE PARAMETERS OF ZINC OXIDE

| Parameter | Wavelength, Å |                      |               |
|-----------|---------------|----------------------|---------------|
|           | SP500         | Ball-Milled<br>SP500 | ASTM<br>Value |
| $a_0$     | 3.249         | 3.250                | 3.249         |
| $c_0$     | 5.205         | 5.205                | 5.205         |

### III. LITERATURE SURVEY

In conjunction with the experimental program we studied the published literature on zinc oxide. The literature search furnished by JPL (ref. 2) provided nearly all the abstracts surveyed. The bulk of this document made it impossible to examine each original article. For this reason, each abstract was categorized as very important, pertinent, interesting, or irrelevant. Most of the abstracts fell in the two middle categories. The basis of the classification was relevance to zinc oxide photolysis.

In general, information on the following aspects was sought.

- (1) Ultraviolet-radiation-induced defect formation
- (2) Rate and spectral nature of induced photoresponses
- (3) Solid state characterization of intrinsic and induced defects
- (4) Surface chemistry and physical processes
- (5) Fundamental solid state properties.

Several important documents, including the LMSC reports (ref. 3 and 4), were reviewed. While we could argue about a number of minor points, we concur with most of the LMSC findings and analyses, with one major exception, namely, mechanical/thermal damage and radiation damage (to visible reflectance) have not been recognized as distinctly different. The fact that different spectral regions are affected by mechanical/thermal treatment versus ultraviolet radiation requires the

IIT RESEARCH INSTITUTE

postulating of different defects for each effect. Had the LMSC group examined the reflectance data in terms of induced spectral absorptance, they would easily have been able to distinguish between mechanical/thermal- and radiation-induced changes. From their data and interpretations, one would readily infer that mechanical/thermal treatments generate the same optical effects as ultraviolet irradiation. Careful comparison of the respective damage spectra should suffice to point up the large qualitative differences involved.

An article by Van Craeynest et al (ref. 5) on thermal yellowing of zinc oxide powders relates closely to our efforts. They compared the optical spectra of two heat-treated batches of analytical-grade zinc oxide powder. Both batches were heated to 920°C for 1 hr. One batch was quenched to room temperature; the other was cooled slowly. Samples of each batch were then heated 1 hr at temperatures between 100 and 800°C. Free zinc concentrations plus reflection and luminescence spectra were measured. The optical data are presented as reflectances relative to magnesium oxide and, very much like the method we describe in this report, relative to untreated zinc oxide powder. After reviewing their own and several other authors' results, they propose an F center associated with a  $\text{Zn}^+$  ion as the defect responsible for the yellow color (b-band) developed in their samples.

At first we did not concur with this interpretation since the same optical behavior can be induced mechanically, in which

case it is difficult to believe that mechanical forces could cause the material to lose oxygen (create anion vacancies). But a more thorough study suggested caution in rejecting Van Craeynest's assignments. Unfortunately, the vague descriptions of their work are obstacles to interpretation of an important contribution. Since our own experiments indicated that the b-band does not bleach, the responsible defect is more complex than a zinc interstitial.

Zelikin and Zhukovskii (ref. 6) reviewed their own work and that of others and concluded that the presence of oxygen is essential to the formation of yellow luminescence centers. Further, an excess of oxygen and some kind of structural defect are necessary to the development of yellow luminescence. Also, the green luminescence band is observed only when oxygen deficiencies exist in the lattice. They claim that the bands are inherent properties; their magnitudes can be enhanced or suppressed by but do not depend qualitatively upon the presence or absence of impurities.

The conclusion regarding green luminescence accords with that of Heiland et al (ref. 7), who associate it with a stoichiometric excess of zinc, which, as they suggest, serves as the activator. Likewise, these authors agree that the yellow luminescence center is a zinc deficiency.

Collins and Thomas (ref. 8) conclusively established the effect of oxygen pressure on photoconduction. They proposed that holes from hole-electron pairs discharge lattice oxygen



ions at the surface, and thus a surface excess of zinc and an electron-enrichment layer in which conduction occurs are produced. They measured the quantum efficiency of the ultraviolet absorption process, i.e., the number of conduction electrons formed per incident ultraviolet photon. The quantum efficiency starts at about 0.25 and drops several orders after exposure to  $\sim 10^{16}$  photons/cm<sup>2</sup> ( $\lambda < 3650$  Å). Interestingly enough, their work also demonstrated reciprocity in photoconductance and indicated that the spectral quantum efficiency curve follows the fundamental optical absorption edge very closely. They propose that the holes from the hole-electron pairs produced by the ultraviolet absorption action diffuse to the surface and become trapped on oxygen ions, discharging them to form free oxygen. The ability to follow this process through measurements of surface conductivity gives a measure of the rate of creation of defects.

Heiland (ref. 9), Medved (ref. 10), Melnick (ref. 11), Barry and Stone (ref. 12), Gerritsen et al (ref. 13), and Thomas and Lander (ref. 14) confirmed that the ultraviolet-induced changes in zinc oxide are essentially surface effects and that they are clearly related to photoinduced oxygen desorption. Heiland (ref. 9) found a 1/3 to 1/2 power rate dependence of photoconductivity on irradiation intensity. Collins and Thomas (ref. 8) found reciprocity between quantum yield and radiation intensity for very nearly the same irradiation rates and conditions as Heiland's; the explanation may relate to

IIT RESEARCH INSTITUTE

different trap densities and free-carrier lifetimes. Heiland also suggests that the observed photoconductivity occurs in the conduction band and is augmented by conduction in an impurity band electron trap slightly below the conduction band.

Medved (ref. 10) corroborated Melnick's theory (ref. 11) by correlating photoconductivity with oxygen desorption. Cimino et al (ref. 15) obtained the same effect and reached conclusions similar to those of Medved and Melnick. Barry and Stone (ref. 12) confirmed these findings and discussed a model viewing zinc oxide as an n-type semiconductor with interstitial zinc and with oxygen chemisorbed as  $O^-$  and  $O^{--}$ . Although they considered that interstitial zinc plays an important mechanistic role, they did not suggest it is an electron donor, as did Heiland (ref. 9) and Thomas and Lander (ref. 14). We tend to agree with Barry and Stone. Miller (ref. 16) reviewed the work of Medved and others and extended Medved's theory of chemisorption and conductivity.

The experiments of Gerritsen et al (ref. 13) also demonstrated that the free carriers in zinc oxide are electrons; hole motion was not found. They calculated a trap density of  $10^{14}/\text{cm}^3$  for the position of the Fermi level 0.8 eV below the conduction band and of  $10^{17}/\text{cm}^3$  for its position 0.4 eV below the conduction band. The latter value suggests a distortion of the energy levels of the interstitial zinc with increasing defect concentration. Zelikin and Zhukovskii (ref. 6) also briefly discussed this probability but dismissed it for lack of supporting evidence. IIT RESEARCH INSTITUTE

In addition to studies on the fundamental and optical spectra of zinc oxide, many studies on the infrared spectra have been made. Matsushita and Nakata (ref. 17) studied a band at  $1550 \text{ cm}^{-1}$  ( $6.45 \mu$ ) and, from a correlation of free electrons with band shape and intensity, attributed it to zinc vacancies with trapped electrons.

Thomas (ref. 18) also noticed that strong absorption can arise from the presence of free electrons. He measured the free electron concentrations and correlated them with intrinsic absorption in the 1- to  $12\text{-}\mu$  wavelength region. He reported that the absorption coefficient,  $\alpha$ , varies approximately as  $\lambda^3$  for  $\lambda < 5 \mu$  and is less steep for  $\lambda > 6 \mu$ . At any given  $\lambda$ ,  $\alpha$  varies directly as the free electron concentration. Thomas concluded that there is rough agreement between theory and experiment, but further theoretical work is necessary to make a detailed accounting of his data.

Filiminov (ref. 19) observed that infrared absorption increased after removal of surface-adsorbed oxygen. The oxygen was removed by ultraviolet irradiation in a vacuum. He assumed that the desorption of oxygen is accompanied by an increase in the conduction electron concentration due to release of electrons formerly bound to the adsorbed oxygen. In his view the appearance of an infrared absorption band is naturally associated with an increase in the number of conduction electrons. Absorption then would be caused by electron transitions from donor levels to the conduction band or by transitions within this band.

He observed that the depth of local levels caused by excess zinc varies over a wide range, 0.6 to 0.1 eV, within this band. As Filiminov points out, the variable trap depth makes it difficult to predict the frequency of maximum absorption. From his data, however, he concluded that the monotonic increase in absorption with increasing wavelength suggests an intraband transition. This is the effect we will describe later.

In a similar experiment, Miloslavskii and Kovalenko (ref. 20) studied the electrical and the optical properties versus the film thickness. They found a strong surface effect. In attempting to correlate absorption with electrical conductivity through the Drude relationship, they obtained poor agreement at short wavelengths, 1 to 4  $\mu$ . The presence of a clearly expressed maximum at 5.5  $\mu$ , which they attributed to quantum transitions, produced a marked discrepancy in the correlation. They, too, showed a direct proportionality between long-wavelength absorption and electrical conductivity and, as Filimonov did, associated it with conduction-band electrons.

A study by Collins and Kleinman (ref. 21) of the relationships between spectral reflectance at 1 to 45  $\mu$  and free-carrier concentration resulted in an excellent fit to the data. They found that the usual reflectance spectrum of an ionic crystal is observed in samples with free-carrier concentrations below  $10^{16}/\text{cm}^3$ , but that the contribution to the optical constants becomes significant at concentrations in excess of  $10^{17}/\text{cm}^3$ . The authors claim a good fit over the range of

IIT RESEARCH INSTITUTE

1 to 45  $\mu$ . This finding contrasts with that by Miloslavskii and Kovalenko (ref. 20), but the difference may be explained on the basis of the high carrier concentrations in Miloslavskii's work compared to those in the Collins-Kleinman study.

Amberg and Seanor (ref. 22) correlated oxygen absorption and desorption with infrared optical spectra. They followed the free-carrier absorption in the region of 1300 to 1600  $\text{cm}^{-1}$  (7.7 to 6.25  $\mu$ ). They used New Jersey Zinc's Kadox 25 undoped, lithium-doped, and gallium-doped. They ascribe the absorption in this region to free carriers. This assignment differs from that of Kasai (ref. 23) but is in line with those made by Thomas and Lander (ref. 14), Filiminov (ref. 19), Miloslavskii and Kovalenko (ref. 20), and Collins and Kleinman (ref. 21). The apparent conflict stems in part from differences in materials and in interpretations of data.

Because there might be a direct verification by electron spin resonance techniques of our earlier (ref. 24) photolysis postulates, we reviewed several pertinent articles. Kokes (ref. 25) studied the chemisorption properties of zinc oxide prepared by three different methods; one of his materials was New Jersey Zinc's SP500. He used electron spin resonance analysis to show that oxygen chemisorption significantly affects the surface properties of zinc oxide regardless of the method of preparation. His data showed that the electron spin resonance signal directly reflects the concentration of free electrons. He concluded that the low-temperature ( $<400^\circ\text{C}$ ) form of

IIT RESEARCH INSTITUTE

chemisorption occurs as  $O^-$ , whereas at higher temperatures oxygen is in the form  $O^{--}$ . In a later article, Glemza and Kokes (ref. 26) presented the same postulate and offered additional absorption and conductivity data. They also used SP500 as one of their materials.

The results of many electron spin resonance observations on zinc oxide and other Group II-VI semiconductors were summarized by Müller and Schneider (ref. 27). They tabulated the g-values and H (gauss) half-widths reported by many other experimenters. Significantly, they noted the necessity for ultraviolet excitation as a prerequisite to a detectable electron spin resonance signal. Baranov et al (ref. 28) were even more explicit about the necessity of ultraviolet stimulation of electron spin resonance signals. Like Kokes (ref. 25), they found that the ultraviolet-induced electron spin resonance signal persisted after termination of the ultraviolet irradiation. They showed also that ultraviolet irradiation in air had no electron spin resonance effect above 20°C.

The effect of lithium doping was reported by Kasai (ref. 29), who found no preirradiation electron spin resonance signal even in heavily doped zinc oxide. The fact that no electron spin resonance signal can be detected without ultraviolet stimulation is consistent with the findings of other experimenters.

We verified in part the above findings. Samples of SP500 zinc oxide untreated, mechanically yellowed by ball-milling, and doped with lithium in each case gave no detectable electron

spin resonance signal at 77°K. The sensitivity of the procedure is estimated at  $2 \times 10^{16}$  spins. If the lithium had given rise to an unpaired spin, its signal should have been very large, since the doped sample had a concentration of 0.1 mole % lithium. The results accord with those found by Baranov et al and by Kasai.

In a thesis, DeWitt (ref. 30) presented the results of an analytical and experimental study on the optical properties of zinc oxide and cadmium selenide single crystals. He analyzed his data by using the Kramers-Kronig dispersion relations. He reported reflectivity, index of refraction, extinction coefficient, and dielectric constant in the range of 2.5 to 14.0 eV (4500 to 900 Å). The reflectance data showed the fundamental optical absorption edge at 3.30 eV; IITRI data indicated 3.32 eV. The index of refraction had a peak value of 2.4 at 2.30 eV. The reflectance curves showed the existence of at least five small peaks in the 3.5- to 14-eV region and of one large reflectivity peak at 5.22 eV.

Chang (ref. 31) studied the restrahlen reflectance of several coatings, including zinc oxide, in the 2- to 40- $\mu$  region. Zinc oxide exhibited a comparatively narrow restrahlen band between 15 and 26  $\mu$  but maintained about 30% reflectance out to at least 40  $\mu$ . His data showed that the difference between the long- and the short-wavelength limits of the index of refraction is not large. This observation is in fair agreement with that given by Heiland et al (ref. 32) and others.



Our search of the literature was made with the hope of finding theoretical and experimental information regarding ultraviolet absorption mechanisms in zinc oxide. Relationships between known defects and their optical properties were found or at least inferred from the data. The assignments we advanced earlier in this contract, given in IITRI-C6027-16, still apply. In particular, from the data on mechanically yellowed powders, some additional evidence was added to our assignment of the 3850-A (3.2-eV) band as being due in part to interstitial  $\text{Zn}^+$ .

#### IV. EXPERIMENTS AND RESULTS

##### A. Mechanical/Thermal Treatments

Many references are made in the literature to the yellow color of zinc oxide when heated, mechanically ground, or ball-milled. In order to relate these references to zinc oxide photolysis, we prepared a series of SP500 samples by yellowing them in various ways described in the literature and determined the resulting reflectance spectra.

Many authors report the appearance of certain effects in zinc oxide after various treatments and frequently describe a change in color or refer to an optical change. Thus, our interest in reproducing the effects reported in the literature was principally to connect optical properties with others that have received more thorough attention. The effects of mechanical treatment, of high-temperature neutral and reducing atmospheres,

of hydrogen bombardment, and of dopants (e.g., lithium, copper, zinc) were studied in terms of catalysis, photoconductance, diffusion, gas sorption, etc. and may be important. Reflectance and electron spin resonance data were obtained for samples of SP500 zinc oxide that were:

- (1) Mechanically yellowed
- (2) Sintered in air at high temperatures
- (3) Vacuum sintered at high temperatures
- (4) Sintered in a hydrogen atmosphere
- (5) Doped with lithium.

A description of each sample and the measured optical data appear in Table 5.

After preparation, the samples displayed various degrees of yellowing depending upon the nature and the intensity of the treatment. No detectable electron spin resonance signal resulted from any of these treatments.

The reflectance of a treated sample was directly compared with that of SP500 zinc oxide by using the Beckman DK-2A spectrophotometer. The treated sample was placed in the sample port. Freshly prepared, untreated SP500 zinc oxide was placed in the reference port. In this manner, the reflectance ratios ( $R_s/R_0$ ) of treated ( $R_s$ ) to control ( $R_0$ ) samples were obtained.

Figure 2 exemplifies the curves obtained in each case. It also shows the optical density ( $\log_{10} [R_0/R_s]$ )<sup>\*</sup> curve resulting when the ratio  $R_s/R_0$  is unity at  $0.7 \mu$ . This curve gives a

Table 5

## MECHANICALLY/THERMALLY TREATED ZINC OXIDE

| Temp.,<br>°F | Time,<br>hr | Atmosphere          | Weight<br>Loss, % | Peak,<br>Å | OD at Peak,<br>$\log_{10} (R_0/R_s)^*$ | g-Value,<br>eV |
|--------------|-------------|---------------------|-------------------|------------|--|----------------|
| 1400         | 1           | Still air           | 0.18              | 3795       | 0.1555                                 | 0.06           |
| 1600         | 1           | Still air           | 0.16              | 3840       | 0.366                                  | 0.18           |
| 1800         | 1           | Still air           | 0.32              | 3825       | 0.518                                  | 0.28           |
| 1800         | 10          | Still air           | 0.35              | 3850       | 0.520                                  | 0.18           |
| 1800         | 1           | H <sub>2</sub> + Ar | 9.49              | 3860       | 0.208                                  | 0.12           |
| 1000         | 1           | H <sub>2</sub> + Ar | 0.17              | 3775       | 0.035                                  | -              |
| 1400         | 1           | H <sub>2</sub> + Ar | 1.35              | 3850       | 0.205                                  | 0.11           |
| 1600         | 1           | H <sub>2</sub> + Ar | 2.47              | 3845       | 0.272                                  | 0.11           |
| -            | 24          | Ball-milled         | -                 | 3875       | 0.469                                  | 0.47           |
| -            | 48          | Ball-milled         | -                 | 3875       | 0.600                                  | 0.53           |
| -            | -           | 0.01 mole % Li      | -                 | 3790       | 0.127                                  | 0.20           |
| -            | -           | 0.10 mole % Li      | -                 | 3790       | 0.0975                                 | 0.18           |

\* Refers to reflectance normalized at 0.7  $\mu$ .

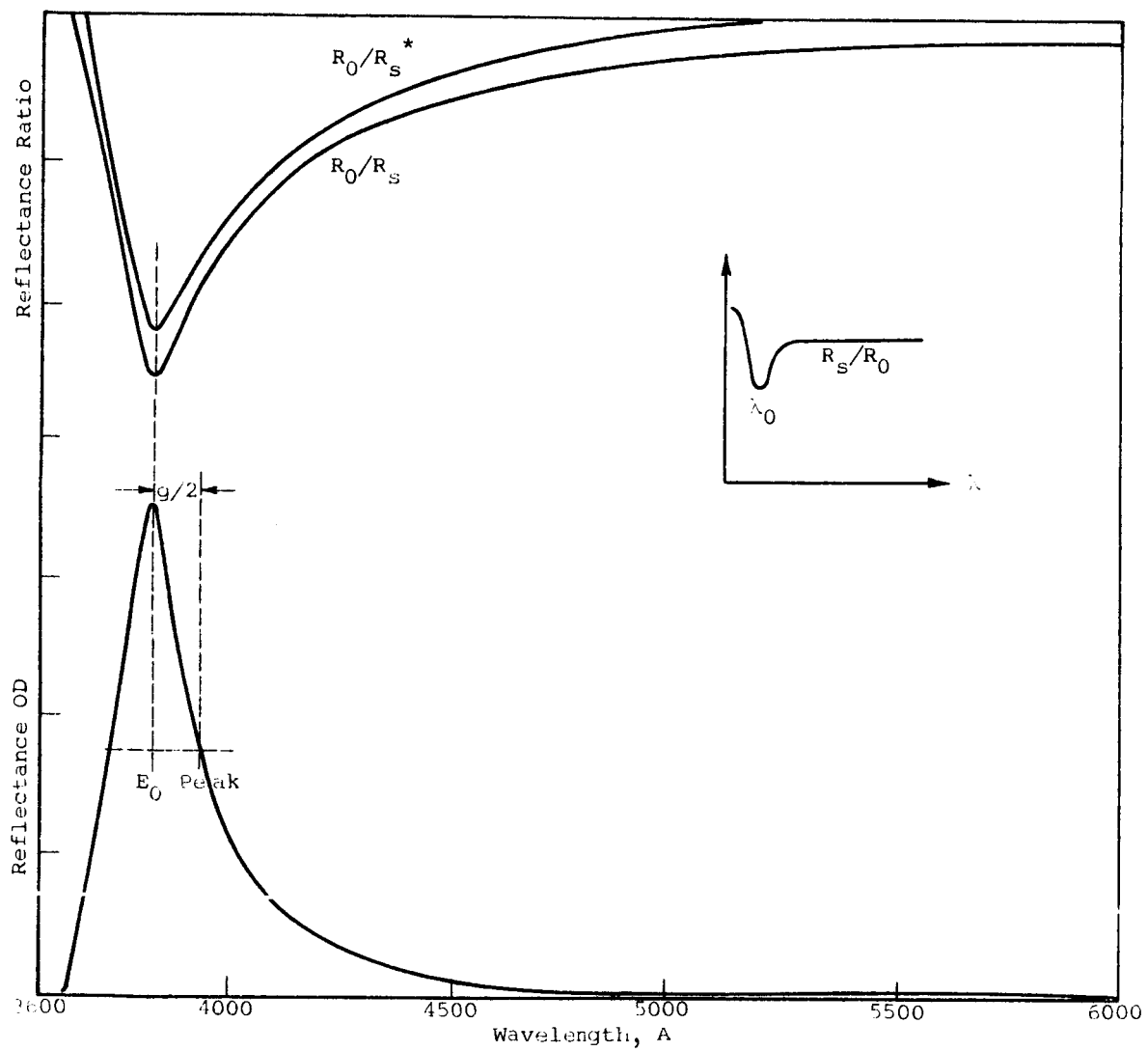


Figure 2  
GENERALIZED MECHANICAL-THERMAL DAMAGE SPECTRA

much clearer representation of the absorption induced by the treatment, since the process of normalizing at  $0.7 \mu$  merely removes the effects due to differences in particle size, degree of compaction, and other geometrical properties, even thickness. (All samples were a minimum of 0.025 in. in thickness.) The validity of this process was confirmed with each sample by comparing the actual value of  $\log_{10} (R_0/R_s)$  at  $0.7 \mu$  with the difference between actual and normalized optical densities at the peak.

The reflectance data in Figure 2 and Table 5 clearly indicate the essential difference between damage induced by ultraviolet (and other energetic) radiation and that induced by mechanical and thermal treatment. Whereas ultraviolet radiation induced damage at wavelengths above  $0.70 \mu$ , mechanical and thermal treatments induced damage at  $0.37$  to  $0.38 \mu$ . Mechanical/thermal effects are intrinsically different from radiation effects.

Table 6 shows the resolution attained by the Beckman DK-2A spectrophotometer in the region of  $0.36$  to  $0.70 \mu$ . Magnesium oxide data are given for comparison. It is easy to see that the spectral resolution is more than sufficient to isolate the b-band.

The most likely defect responsible for absorption at  $3850 \text{ \AA}$  is interstitial zinc. This assignment is favored over others because, in addition to more fundamental reasons, it can account for the induced reflectance increase at wavelengths below the fundamental absorption edge (see inset in Figure 2).

IIT RESEARCH INSTITUTE

Table 6

## SLIT CONTROL AND SPECTRAL RESOLUTION OF THE BECKMAN DK-2A SPECTROPHOTOMETER

| Wavelength,<br>$\mu$ | Half Bandwidth,<br>$m\mu/mm$ slit width | Zinc Oxide          |                       | Magnesium Oxide     |                       |
|----------------------|---|---------------------|-----------------------|---------------------|-----------------------|
|                      |   | Slit Opening,<br>mm | Resolution,<br>$m\mu$ | Slit Opening,<br>mm | Resolution,<br>$m\mu$ |
| 0.700                | 50                                      | 0.43                | 43                    | 0.44                | 44                    |
| 0.600                | 33                                      | 0.05                | 3.3                   | 0.05                | 3.2                   |
| 0.500                | 20                                      | 0.037               | 1.5                   | 0.04                | 1.6                   |
| 0.400                | 9                                       | 0.16                | 3.2                   | 0.155               | 2.8                   |
| 0.370                | 8                                       | 0.62                | 9.9                   | 0.28                | 4.4                   |
| 0.365                | 7                                       | 2.00                | 14                    | 0.45                | 6.2                   |
| 0.350                | 6                                       | >2.00               | 5.0                   | 0.50                | 6.0                   |

<sup>a</sup>At maximum amplifier gain (sensitivity).

The  $R_s/R_0$  spectra consistently showed a value greater than unity at wavelengths below  $0.37 \mu$ . This behavior precludes the judgment that such an effect is apparent rather than real. The spectra below the edge cannot be considered quantitatively significant since the slit width reaches a maximum at  $0.355 \mu$ . Interestingly enough, the b-band parameters in lithium-doped zinc oxide do not reflect lithium concentration.

Samples of untreated SP500 zinc oxide, zinc oxide ball-milled for 48 hr, and zinc oxide doped with 0.1 mole % lithium were irradiated in air to a total dose of about 150 equivalent solar-hours. The untreated sample displayed no measurable change in spectral reflectance; the ball-milled and lithium-doped samples did. The b-bands appeared to have bleached and broadened as a result of the irradiation.

Analysis of the induced absorption curve of the 48-hr ball milled zinc oxide indicated that the band has a classical Lorentzian shape. The fit to the actual curve shape was excellent when the dispersion of the index of refraction,  $n$ , was taken into account. From Heiland et al (ref. 7) we obtained the experimental refractive index data and found that they could be well represented by the expression:

$$n^2 = 4.128 - 0.1334 E^2 + 0.02453 E^4$$

where

$E$  is photon energy.

Using this expression, we determined the Lorentzian oscillator parameters:  $E_0 = 3.230$  eV;  $g = 0.51$  eV.

IIT RESEARCH INSTITUTE



## B. Luminescence

The photoluminescence of mechanically/thermally yellowed zinc oxide powders was studied. The object was to determine whether there is a relationship between the mechanically/thermally induced absorption band at 3850 Å and the luminescence peaks. No attempt was made to establish the absolute magnitudes of the luminescent intensities.

The data were obtained with an Aminco-Keirs spectro-phosphorimeter, which incorporates a Xenon excitation source, two grating monochromators, and a detector. A band of the excitation spectrum, selected by one monochromator, induces luminescence, which is analyzed by the second monochromator.

The excitation light was 2750 Å. Luminescence scans were made in the region from 4000 to 8000 Å. The powder film was always oriented on the luminescence detector side, with the substrate (glass) on the excitation side. A series of seven SP500 zinc oxide samples was prepared by spraying slurries on ordinary laboratory glass slides. The thickness of the deposited film was controlled approximately by selecting specimens with a nominal 50% transmission at 4360 Å.

The luminescence data are summarized in Table 7, and the spectral data are shown in Figure 3. The spectral data can be assumed to have 20% accuracy in relative intensity. Mechanical treatment produced longer and different wavelength effects from those produced by thermal treatment. Doping and heating increased short-wavelength (4600 to 4700 Å) luminescence without altering emission at 5000 Å.

IIT RESEARCH INSTITUTE

Table 7  
LUMINESCENCE OF VARIOUS ZINC OXIDE SAMPLES

| Sample  | Relative Intensity |                   |        |                        |               |
|---|--------------------|-------------------|--------|------------------------|---------------|
|   | 460/470 mμ         | 500 mμ<br>(Green) | 565 mμ | 615/620 mμ<br>(Yellow) | 625 mμ 635 mμ |
| Untreated   | -                  | 0.006             | -      | 0.39                   | - -           |
| Ball-milled 48 hr                                     | -                  | 0.003             | -      | -                      | 0.023         |
| Ball-milled 100 hr                                    | -                  | 0.003             | -      | -                      | 0.026         |
| Li-doped 0.01 mole %                                  | 0.032              | -                 | -      | 0.66                   | 0.12          |
| Li-doped 0.1 mole %                                   | 0.025              | -                 | -      | 0.55                   | 0.093         |
| Heated at 1400°F in<br>H <sub>2</sub> and Ar for 1 hr | 0.026              | -                 | -      | -                      | 0.44 -        |
| Heated at 1400°F in<br>air for 1 hr                   | 0.026              | -                 | 0.06   | 0.47                   | - 0.069       |

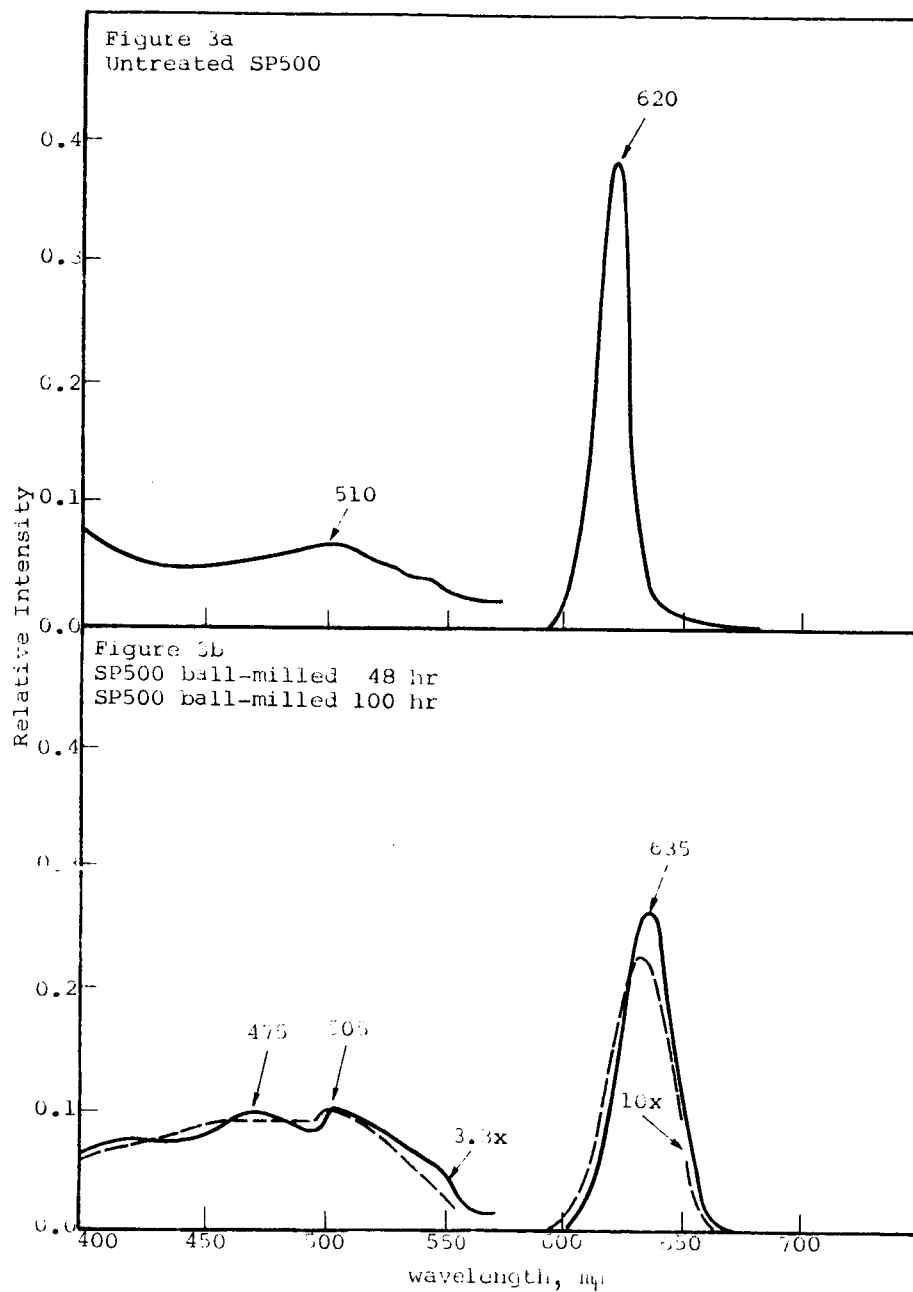


Figure 3  
LUMINESCENCE SPECTRA OF VARIOUS ZINC OXIDE SAMPLES  
AT 2750-Å EXCITATION

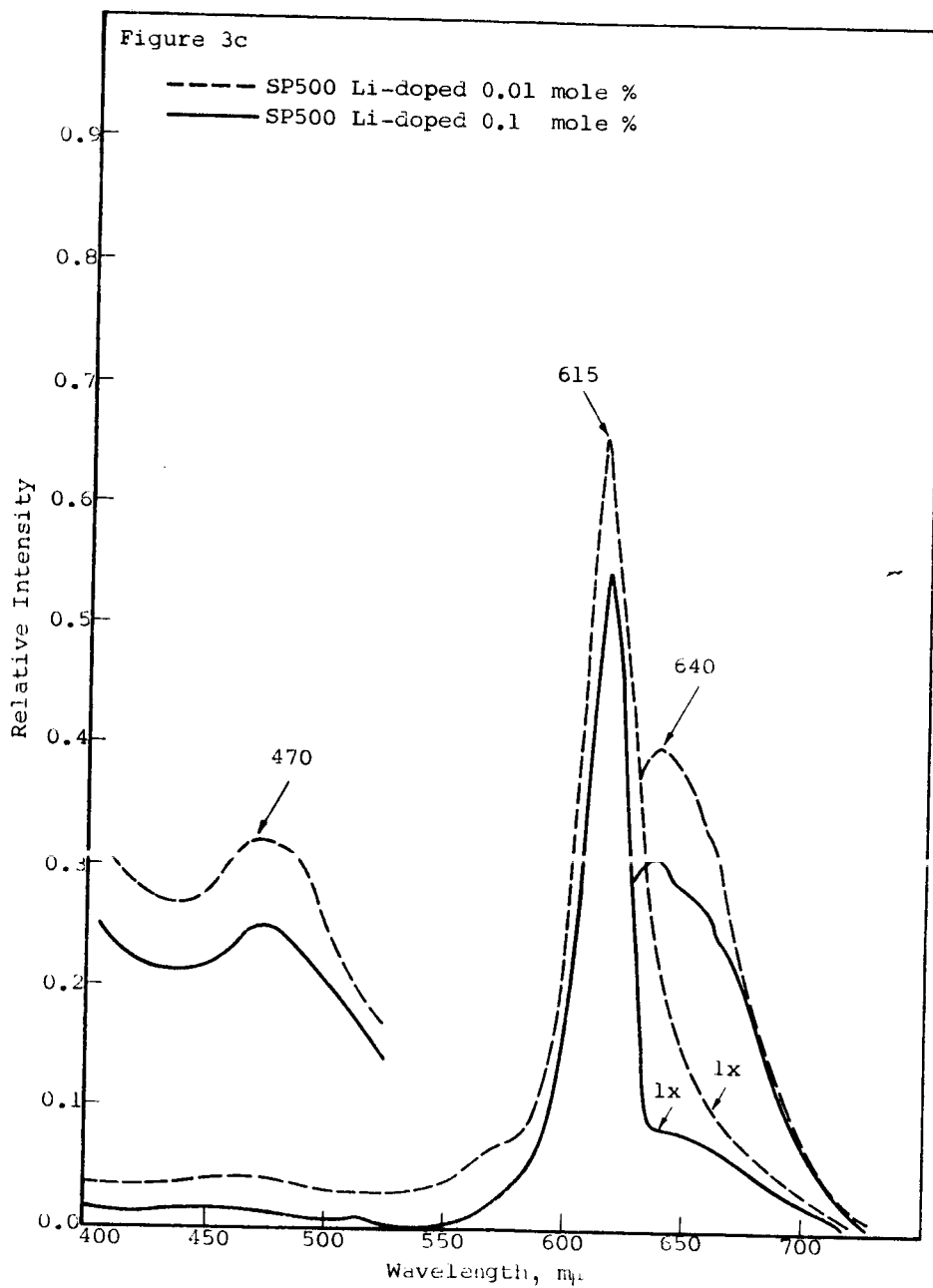


Figure 3 (cont.)

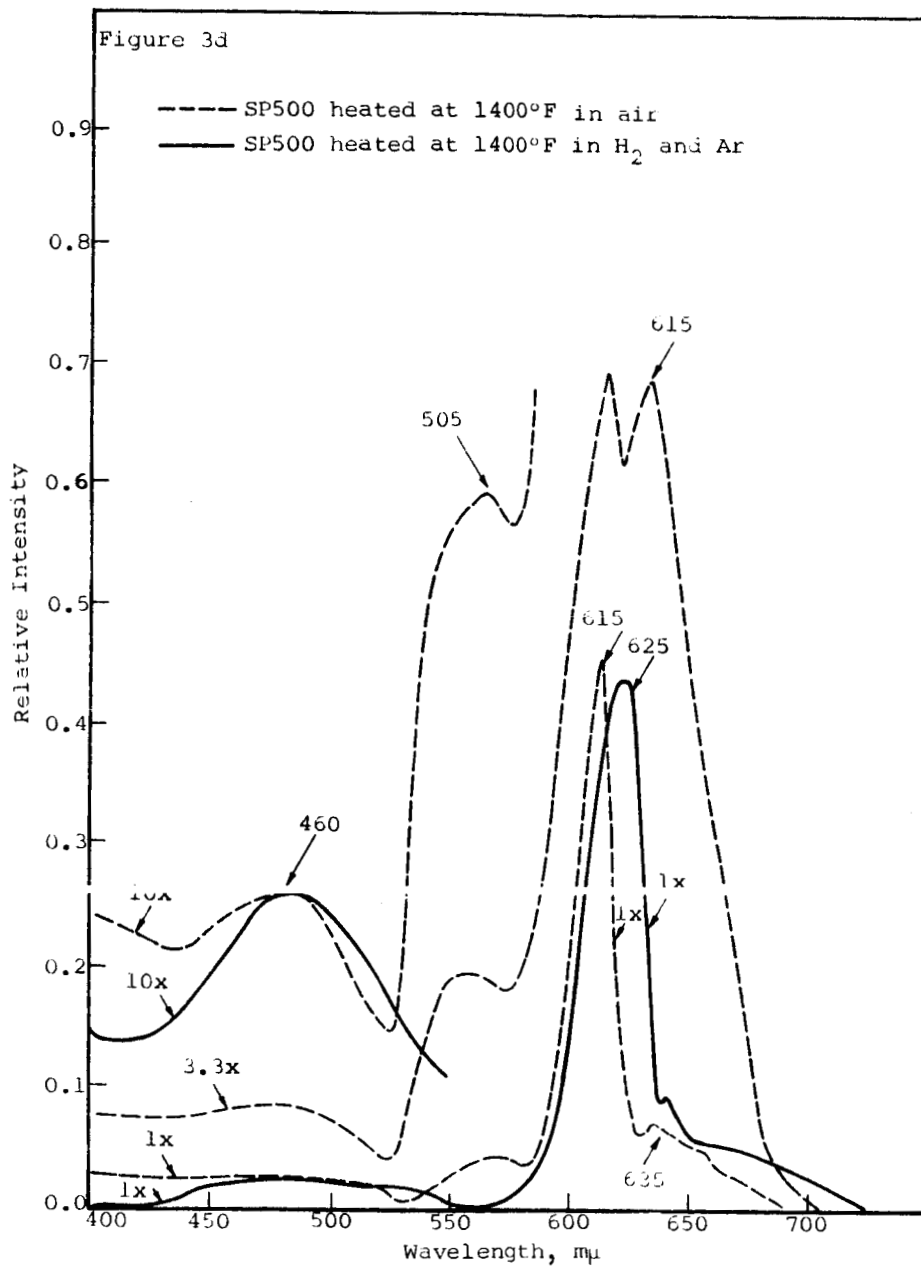


Figure 3 (cont.)

A significant, though not yet understood, point is that luminescence does not follow lithium concentration. In fact, the trend is opposite to what would be expected. Yellow luminescence apparently does depend upon pretreatment. The data concerning the importance of the role of interstitial zinc in electron-hole recombination processes in zinc oxide are not conclusive. The lithium dopant data suggest augmented recombination; but, if it is assumed that the lithium is in interstitial sites, then  $\text{Zn}^+$  interstitials should also promote recombination. The data on the heated samples do not conflict with this view, but neither do they support it.

A fair summary of these findings is that the luminescence curves indicate that interstitial zinc may indeed be involved in the yellow luminescence scheme but not in the green luminescence scheme. Additional data are necessary to determine the effect of interstitial zinc in recombination processes. Mollwo (ref. 33) suggested that a diffusing species can account for the quenching of green luminescence when zinc oxide is heated in hydrogen. The present data do not confirm this view, but neither do they preclude its consideration. Lithium had an effect in the expected direction, if interstitial diffusion were important, but not nearly as small an effect as that of hydrogen. The data clearly show the large influence of sample treatment on luminescence spectra but do not necessarily reveal a causal relation between interstitial zinc and the recombination processes.

The luminescence spectra also show that:

- (1) Untreated SP500 zinc oxide luminesces strongly.
- (2) The intensity of yellow luminescence (615/620 mμ) apparently relates to oxygen.
- (3) None of the luminescence bands relate to the b-band (3850 Å), since neither the luminescence intensity nor its spectral location correlate with height, spectral location, or g-value of the b-band.
- (4) The similarity of luminescence spectra of lithium-doped, hydrogen-treated, and air-treated samples suggests that the same trapping defect is common to all three. On the other hand, the traps in ball-milled zinc oxide generally disappeared after the treatment. Comparison of the mechanical/thermal treatment data with the luminescence data suggests that the energy levels of the defects created by mechanical treatments are broader than those due to thermal treatments. We can infer that the broader absorption in the mechanical case results from a less complex center.

From the fact that all treatments except the ball-milling produce essentially a bulk effect, we can conclude that the large quantitative differences between the ball-milled samples and the other treated samples result from surface versus bulk effects. The much larger g-value (broader absorption) in the

b-band of ball-milled samples certainly aids this conclusion. Hence, the comparison of luminescence and b-band spectra emphasizes the differences between surface and bulk effects. We might speculate that ball-milling produces a severe distortion of surface levels, while the other treatments effect more uniform changes in the crystal. Thus, the expectation would be that the internal changes would be higher in energy and show fewer and more discrete energy levels. Surface states would be less in number and in energy (longer wavelength). The data support these predictions but are by no means conclusive.

### C. Proton Irradiation

An experiment in which an S-13 paint sample (35% pigment volume concentration of New Jersey Zinc SP500 zinc oxide in General Electric's RTV-602) was exposed to low-energy protons confirmed an earlier hypothesis that hydrogen treatment and low-energy proton irradiation produce the same qualitative effect. The sample was exposed to more than  $10^{16}$  protons/cm<sup>2</sup>. A normal spectral reflectance measurement in the ratio mode showed that the damage spectrum is identical with that induced by thermal/mechanical treatment.

The fact that protons cause defects identical in optical effect to those generated by mechanical/thermal treatment, but clearly different from those occasioned by ultraviolet irradiation, implies that proton and ultraviolet radiations create defects that are fundamentally different and distinguishable. Infrared bleaching, however, was not investigated.

IIT RESEARCH INSTITUTE



#### D. Induced Infrared Absorption

The behavior of zinc oxide subjected to ultraviolet illumination in vacuo was studied. We conclusively showed that photoinduced properties are dependent on the surface pressure of adsorbates. In studying the in situ reflectance of zinc oxide we also found several interesting effects relating to photodesorption, reflectance recovery, and gaseous adsorbates.

To observe the changes induced by ultraviolet, an apparatus was used in which a sample can be irradiated in a high vacuum and spectral reflectance measured without disturbing the sample or the vacuum environment. Figure 4 illustrates the essential features of the apparatus.

In each test the reflectance scan was made before installation of the sample in the exposure rig, after installation but before evacuation of the rig, after pumpdown to less than  $10^{-5}$  torr, and subsequently after ultraviolet illumination, temperature increases, infrared exposures, and exposure to air, nitrogen, or argon atmospheres, etc.

In most of the experiments zinc oxide dust coatings on aluminum were used. In every instance the environmental pressure at the sample was reduced to and maintained at less than an estimated  $10^{-5}$  torr (maximum) prior to and during ultraviolet illumination. Ultraviolet exposures on separate samples were varied from 0.05 to 500 equivalent solar-hours.

The effect of ultraviolet irradiation upon zinc oxide powders was a decrease in infrared reflectance. The magnitude

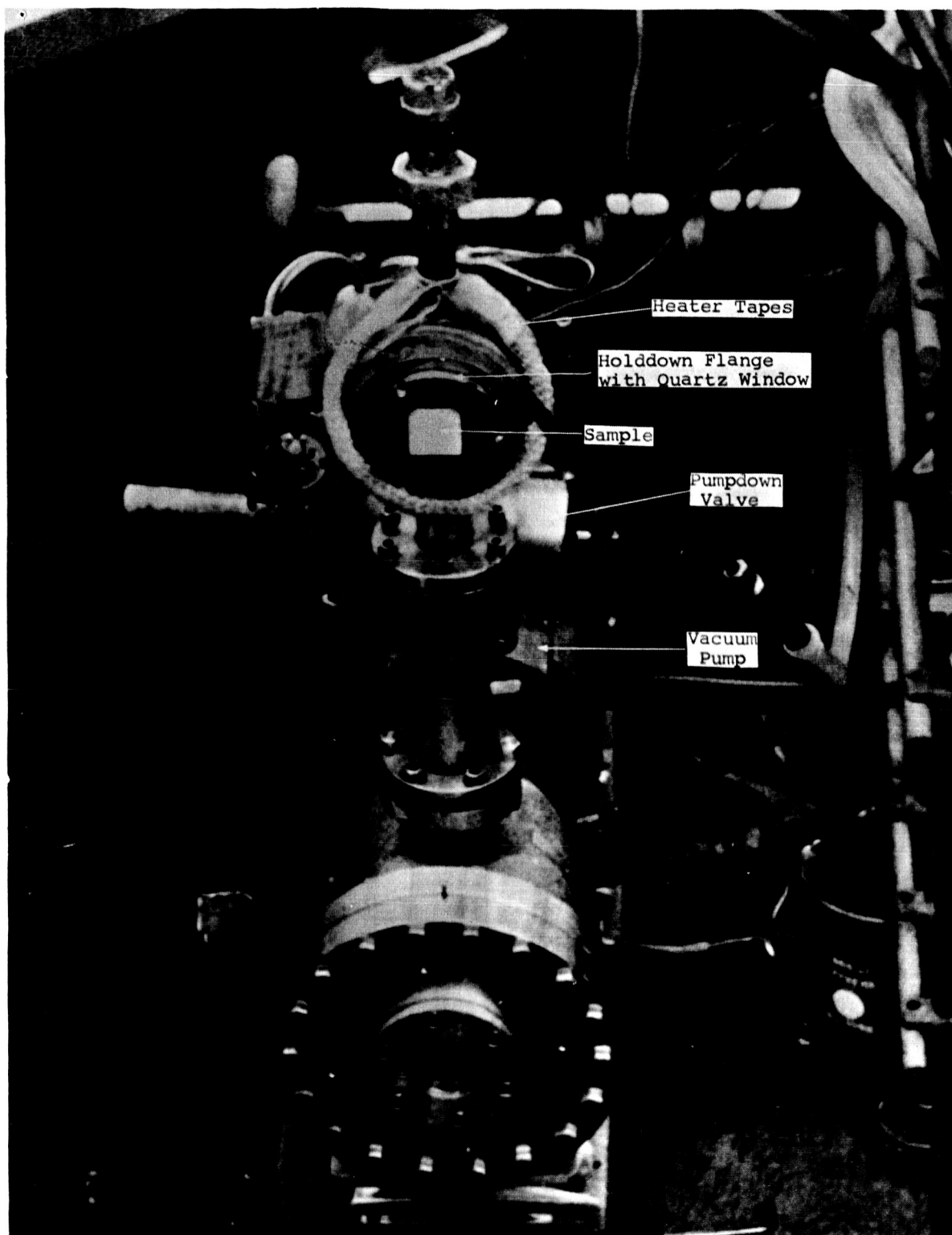


Figure 4

ULTRAVIOLET IN SITU REFLECTANCE APPARATUS

of the induced change increased with increasing wavelength. The effect could be induced in exposures of 0.05 equivalent solar-hour. Figure 5 shows typical reflectance spectra recorded in several experiments.

In a series of tests on SP500 zinc oxide the following observations were made.

- (1) Prior to any treatment, the OD curves for atmospheric pressure and for  $10^{-5}$  torr differed only very slightly. Pumpdown did not affect the reflectance of virgin samples.
- (2) Upon ultraviolet irradiation, the OD increased considerably. The magnitude could not be directly correlated with absorbed dose. The system pressure rose slowly during irradiation and leveled off after intervals of the order of minutes.
- (3) After ultraviolet illumination, the infrared reflectance could be restored to its original value by admitting air, and the damage spectrum generated by ultraviolet could be regenerated merely by reevacuating the test chamber -- a "memory" effect that has been observed over several cycles of vacuum and air exposure.
- (4) When air was readmitted, the reflectance spectrum recovered its preirradiation value almost instantaneously -- better than 80% in less than a second and the remainder in less than a minute.

IIT RESEARCH INSTITUTE

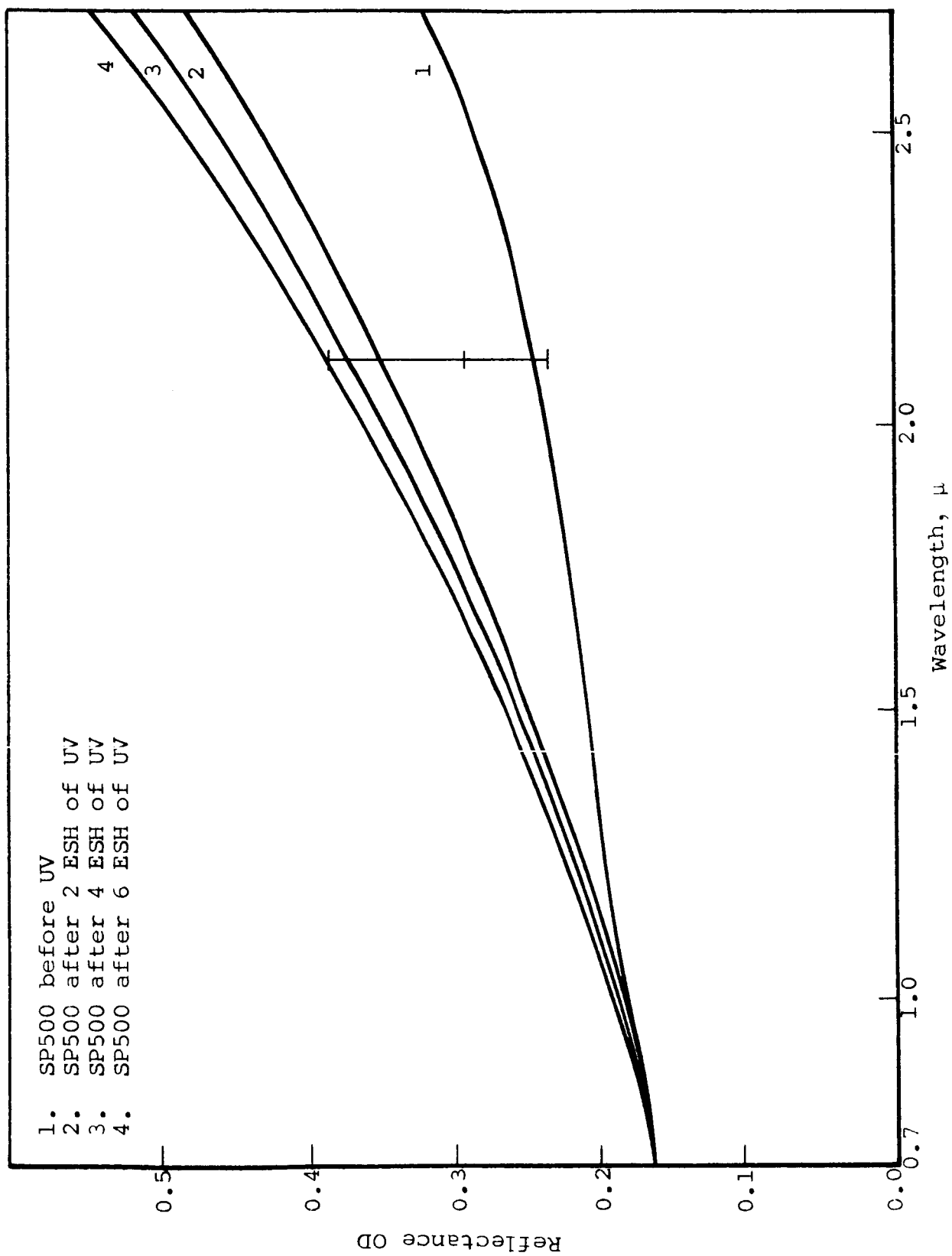


Figure 5

REFLECTANCE SPECTRA OF VARIOUS ZINC OXIDE SAMPLES

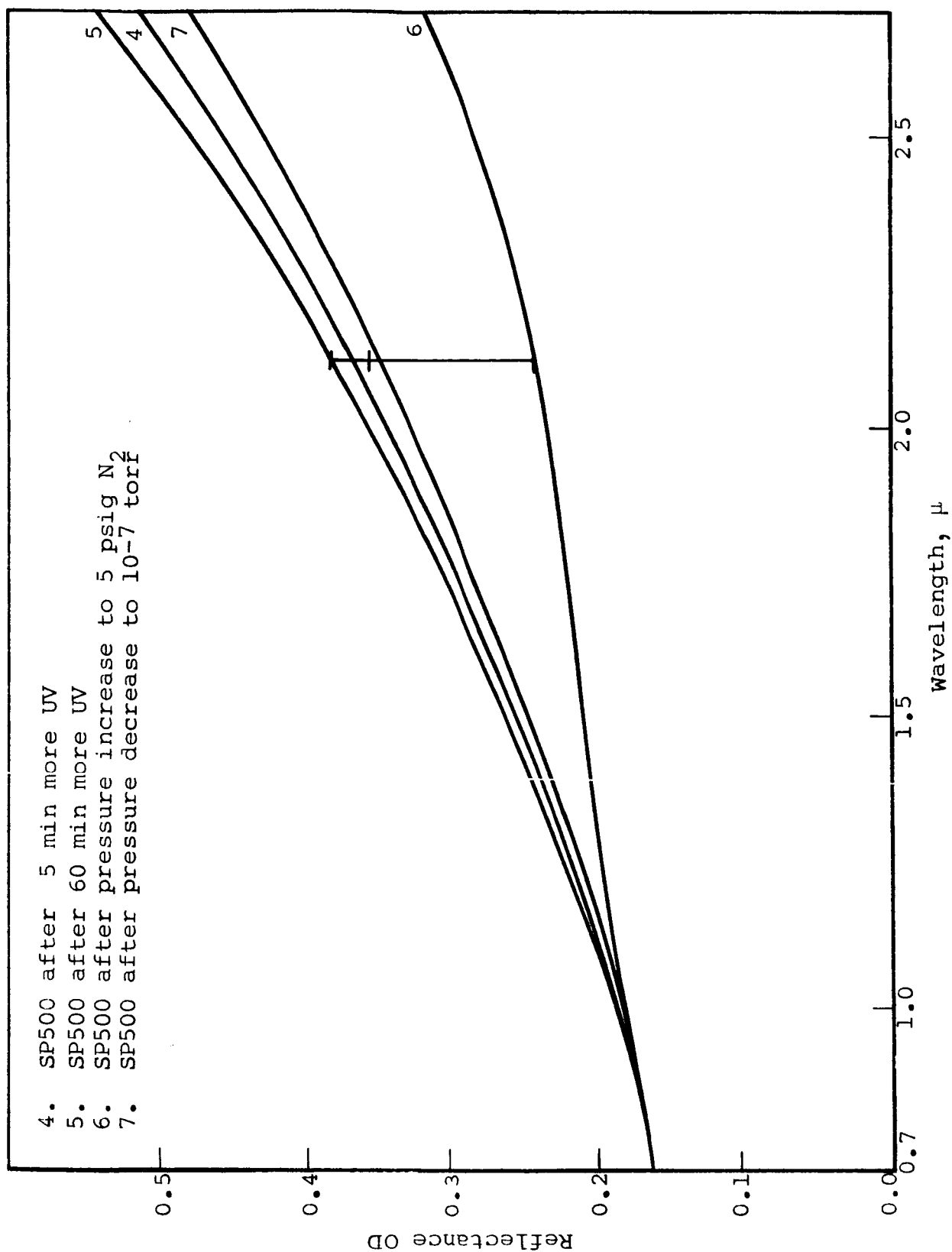


Figure 5 (cont.)

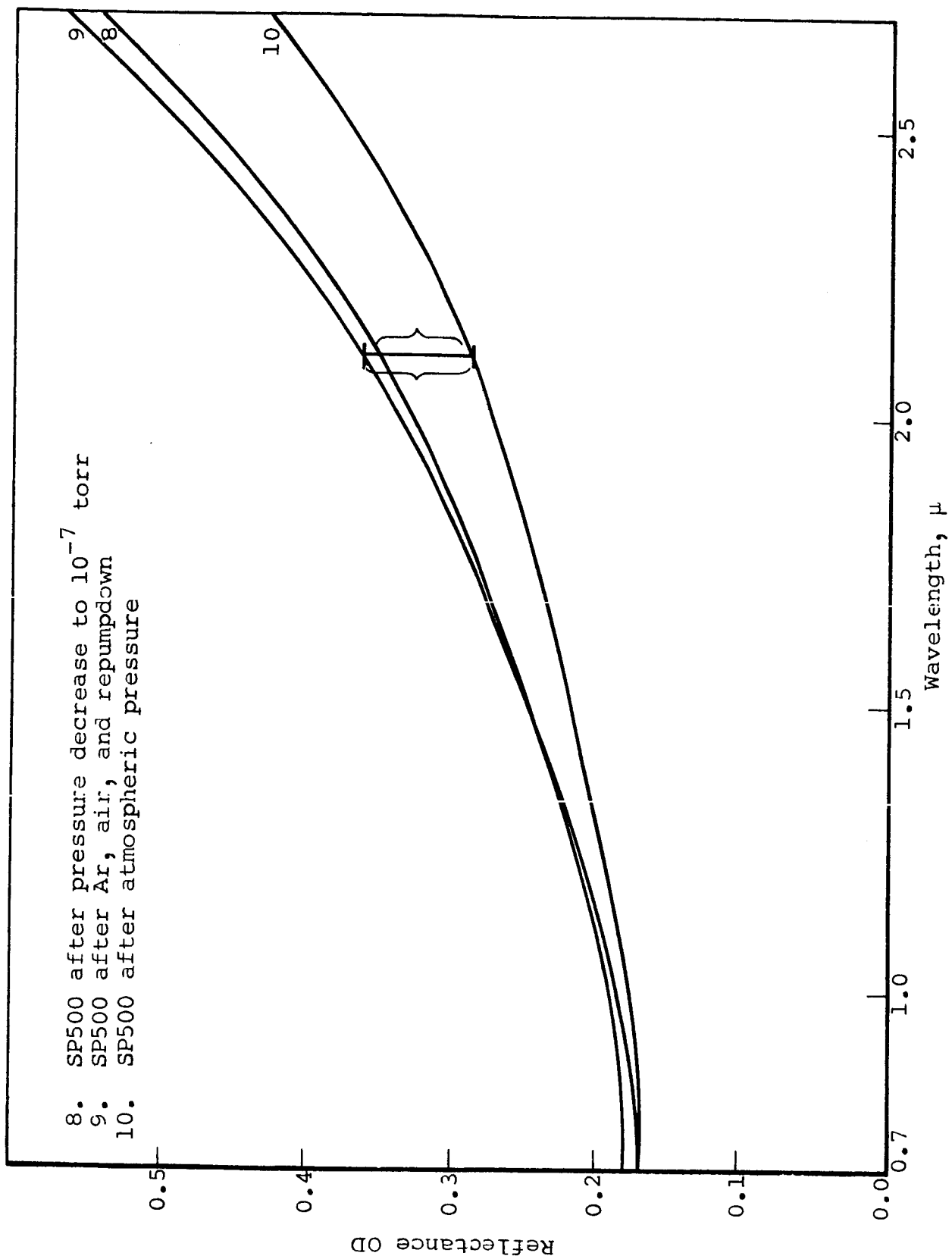


Figure 5 (cont.)

Longer times were required when paint systems, e.g., S-13, were tested, presumably because of diffusion effects.

- (5) When pure nitrogen was admitted, the reflectance nearly recovered its original value. The recovery rate was similar to that when air was admitted. Again, however, a time of the order of minutes was required to recover fully -- during which time some oxygen may enter the system. Argon produced no effect; a pressure of 5-psig argon held for 5 min did not affect the ultraviolet-induced reflectance.
- (6) Temperatures up to 400°F did not induce infrared changes in otherwise untreated samples.
- (7) Broad-spectrum infrared radiation did not affect the ultraviolet-induced infrared damage.
- (8) After illumination with ultraviolet, a major fraction of the reflectance change in zinc oxide became reversible. That is, the ultraviolet-induced loss in reflectance in the infrared was almost fully recovered by admitting air to the system, and the original loss was regenerated simply by reevacuating the system. This "memory" effect was observed over a minimum of 2 cycles.

- (9) Intermittent measurements of successive irradiations indicated that a substantial fraction of the reflectance loss occurred within less than 0.05 equivalent solar-hour of exposure.
- (10) Lithium-doped zinc oxide samples did not display any photoinduced infrared effects.
- (11) After prolonged exposure, only a partial instantaneous reflectance recovery occurred when nitrogen was admitted. Over a period of 5 to 7 min the reflectance recovered fully, possibly because oxygen leaked into the system. This behavior contrasts with the nearly complete instantaneous recovery experienced when air was admitted. The "memory" effect may still be operative, but the amount of reversible change is that which is first seen instantaneously with nitrogen. The reversible effect relates to the loss and gain of physically adsorbed gases.

The infrared reflectance degrades in zinc oxide as a result of the loss of adsorbed gases, that is, because of photodesorption. In particular, our observations can be reasonably well explained on the assumption of a free-carrier absorption scheme. OD spectra strongly support this contention. Further evidence comes from the fact that the photodesorption occurs extremely rapidly.



The literature contains many accounts either directly or indirectly pertinent (ref. 8, 10-12, and 18). The most popular thesis holds that two types of adsorption can occur on zinc oxide: physical adsorption and chemisorption. In the first case, adsorbed oxygen is held by a weak, one-electron bond; in the latter, by a two-electron bond. Irradiation causes the more loosely bound oxygen to be desorbed quickly (ref. 8, 25, and 26). The chemisorbed oxygen, of course, also desorbs but very much less rapidly.

The mechanisms operating to produce the infrared effect remain somewhat in doubt, but it seems certain that the absorption results from intraband transitions of electrons in the conduction band. The conduction band electron concentration in an intrinsic semiconductor ordinarily depends upon temperature and the position of the Fermi level. When donor impurities are present, however, the free-electron concentration can be greatly increased. In the present case, the free-electron concentration increased when adsorbed gases captured holes generated by the ultraviolet radiation.

#### V. SUMMARY AND CONCLUSIONS (THE PHOTOLYSIS SCHEME)

The facts and observations at hand were analyzed to determine the most likely explanation for the photolytic behavior exhibited by zinc oxide. Our principal concern was to define the mechanisms involved in the formation of the two major optical defects in zinc oxide: the 3850-A band and the

induced infrared absorption system. Although the defect structure responsible for the 3850-A band has been studied by a number of investigators, there is considerable doubt about its structure and formation. Our most recent data, though not quantitatively accurate, do not show a definite connection between the 3850-A band and the infrared system.

The infrared absorption system is not yet fully understood either, but far more information about its structure and origin has been accumulated than about the 3850-A system. The ultraviolet photolysis scheme is by no means simple. To understand it even modestly we must resort to band theory and to quantum mechanical ideas about energy structures in matter.

In its usual form, zinc oxide is an n-type semiconductor, and it inevitably displays considerable band curvature due to trapped surface charges. Figure 6 is a typical representation of this band structure. The process of fundamental absorption in zinc oxide causes an electron to enter the conduction band and to leave a hole in the valence band. The upward curvature of the bands arises from bound negative charges at or near the surface and the resultant electric potential. As long as this curvature exists, the valence band holes are attracted (accelerated) to the surface, where they discharge adsorbed gases by capturing their electrons. This process can continue only as long as there are hole traps (adsorbed gases) at the surface. But as the surface charge is depleted, the holes no longer are strongly attracted, and band curvature disappears. Figure 7 illustrates this effect.

IIT RESEARCH INSTITUTE

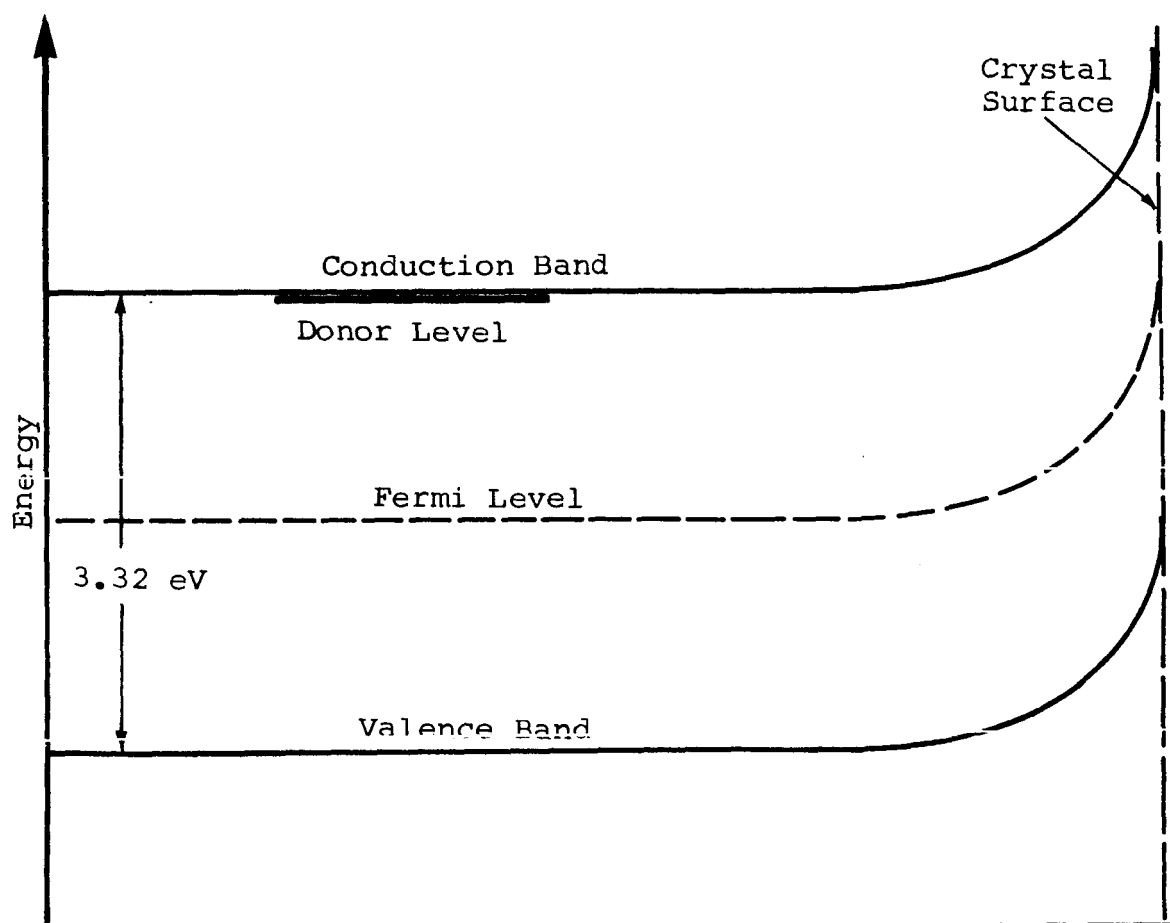


Figure 6  
ELECTRONIC BAND STRUCTURE OF ZINC OXIDE

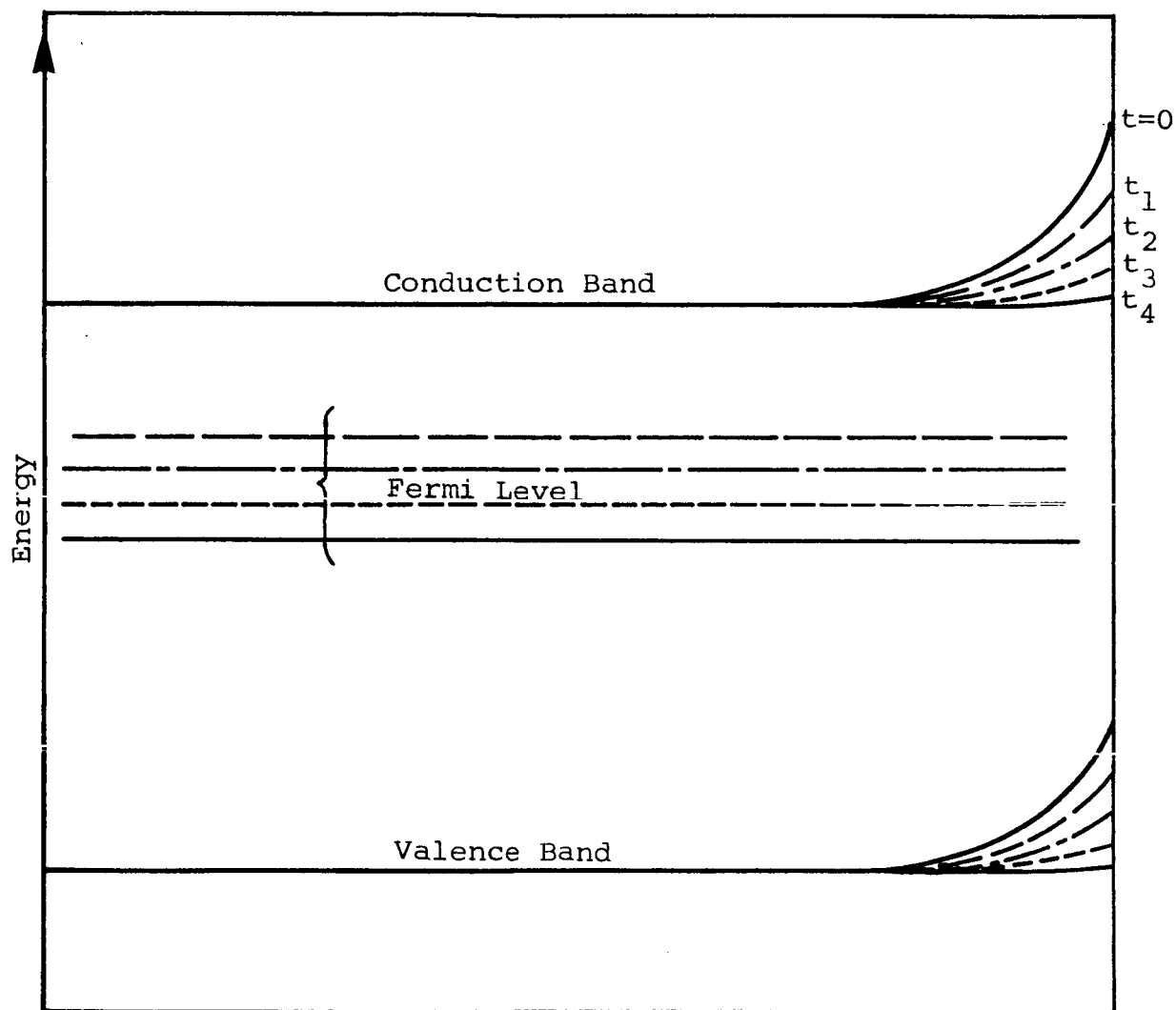


Figure 7

ULTRAVIOLET-INDUCED DEPLETION OF BAND CURVATURE

This process accounts for the nonrecombining holes during the time when band curvature diminishes, but it is important to determine the rate of electron accumulation in the conduction band. Photoconductivity experiments indicate a constantly decreasing photocurrent as illumination continues. Thus, we can argue that direct recombination and other short-lifetime processes become dominant. The reason that recombination is not completely dominant is that when the hole-electron pair is first formed the hole rapidly moves away from the immediate site of the absorption to the surface under the strong influence of the surface potential. In other words, the high concentration of hole traps at the surface compared to the instantaneous concentration of electrons in the conduction band at modest irradiation levels produces a large competitive cross section for surface hole trapping. Recombination still predominates, however.

When the holes combine with the electrons of adsorbed gases, the nonrecombined electrons in the conduction band must either accumulate there or fall into traps. The release of adsorbed gases, as we have seen, causes the infrared absorption to increase. Experimental data indicate that the induced infrared effect reaches a saturation (or equilibrium) value after prolonged ultraviolet irradiation.

Since a very large fraction of the maximum induced change occurs in a very short period of time, the interpretation can be advanced that the principal and critical ultraviolet effect

is that of desorbing physically adsorbed gases (oxygen and nitrogen). The electron that would otherwise have recombined with the hole that discharged adsorbed gases now becomes effectively trapped in the conduction band unless other traps are available. The number of additional conduction-band electrons thus created should be no more than the number of photodesorbed gas atoms.

The process does not end here, however, because there is the possibility that the holes can discharge chemisorbed oxygen and normal lattice oxygen ions. Hence, we can expect a further increase of untrapped electrons in the conduction band, but at a decreasing rate. In any real crystal, of course, many effects exist. Thus, not all free electrons that do not get recombined remain in the conduction band. Anion vacancies, for example, attract electrons because of their double positive charge. Accordingly, the oxygen vacancies that capture electrons become singly charged but still are able to attract electrons.

The first configuration is analogous to an F center in alkali halide notation, and the second configuration to an F' center. Both configurations would be expected to have excited states and, accordingly, to cause additional absorption. Provided the energy separations between states were small or nearly overlapping, a significant amount of nonbleaching infrared absorption would be expected in the case of oxygen traps.

Nevertheless, it is still not certain what defect raises the infrared absorption of ultraviolet-irradiated zinc oxide. The experimental data suggest two time constants of the infrared effect; the rapidity with which it vanishes upon increasing the atmospheric pressure and the "memory" effect must be associated with a permanent removal of the band curvature. This possibility conflicts, however, with the notion that the band curvature arises from a high electron concentration bound to adsorbed gases. A second possibility is that electrons, once freed from the surface, have no further potential drive to return them to the surface even though oxygen or other gases may be there to trap them. Hence, we would expect that the free electrons would absorb heavily in intraband transitions and cause increased infrared absorption. This behavior was observed.

## REFERENCES

1. Hogle, D. H., Personal communication, Electrical Products Div., 3M Co., St. Paul, Minn.
2. "ZnO: Physical and Optical Properties," compiled by L. Anderson, JPL Literature Search No. 640, Nov. 1964.
3. McKellar, L. A., et al., "Solar Radiation Induced Damage to Optical Properties of ZnO-Type Pigments," Eight-Month Progress Report for Period June 27, 1964 to Feb. 27, 1965, Contract No. NAS8-11266, Report LMSC M-50-65-1, Mar. 26, 1965.
4. McKellar, L. A., et al., "Solar Radiation Induced Damage to Optical Properties of ZnO-Type Pigments," LMSC Report No. M-50-65-2, Sept. 1965.
5. Van Craeynest, F., Maenhout-Van der Vorst, W., and Kekeyser, W., "Interpretation of the Yellow Color of Heat Treated ZnO Powder," Phys. Status Solidi, Vol. 8, pp. 841-846, 1965.
6. Zelikin, Y. M. and Zhukovskii, A. P., "The Yellow Luminescence of Zinc Oxide," Opt. i Spektroskopiya, Vol. 11, No. 3, pp. 397-402, 1961.
7. Heiland, G., Mollwo, E., and Stockmann, F., "Electronic Processes in Zinc Oxide," in "Solid State Physics, Advances in Research and Applications," edited by F. Seitz and D. Turnbull, Vol. 8, pp. 193-323, 1959.
8. Collins, R. J. and Thomas, D. G., "Photoconduction and Surface Effects with Zinc Oxide Crystals," Physiol. Rev., Vol. 112, No. 2, pp. 388-395, 1958.
9. Heiland, G., "Photoconductivity of Zinc Oxide as a Surface Phenomenon," J. Phys. Chem. Solids, Vol. 22, pp. 227-234, 1961.
10. Medved, D. B., "Photodesorption in Zinc Oxide Semiconductor," J. Chem. Phys., Vol. 28, pp. 870-873, 1958.
11. Melnick, D. A., "Zinc Oxide Photoconduction, An Oxygen Adsorption Process," J. Phys. Chem., Vol. 26, pp. 1136-1146, 1957.
12. Barry, T. I. and Stone, F. S., "The Reactions of Oxygen at Dark and Irradiated Zinc Oxide Surfaces," Proc. Roy. Soc., Vol. A255, No. 1280, pp. 124-133, 1960.

IIT RESEARCH INSTITUTE



13. Gerritsen, H. J., Ruppel, W., and Rose, A., "Photo-Properties of Zinc Oxide with Ohmic and Blocking Contacts," *Helv. Phys. Acta*, Vol. 30, No. 6, pp. 504-512, 1957.
14. Thomas, D. G. and Lander, J. J., "Surface Conductivity Produced on Zinc Oxide by Zinc and Hydrogen," *J. Phys. Chem. Solids*, Vol. 2, pp. 318-326, 1957.
15. Cimino, A., Molinari, E., Cramarossa, F., and Chesini, G., "The Relations between Photoconductivity and Photo-desorption of Oxygen in Zinc Oxide," *Rend. Accad. Nazl. Lincei*, Vol. 30, No. 5, pp. 750-753, 1961.
16. Miller, P. H., "The Role of Chemisorption in Surface Trapping," in "Photoconductivity Conference," Atlantic City, N. J., Nov. 1954, edited by R. G. Breckenridge, R. B. Russell, and E. E. Hahn. John Wiley and Sons, Inc., New York City, 1956.
17. Matsushita, J. S. and Nakata, T., "Infrared Absorption of Zinc Oxide and of Absorbed Carbon Dioxide," *J. Chem. Phys.*, Vol. 32, pp. 982-987, 1960.
18. Thomas, D. G., "Infrared Absorption of Zinc Oxide Crystals," *J. Phys. Chem. Solids*, Vol. 10, pp. 48-51, 1959.
19. Filiminov, V. N., "Electronic Absorption Bands of ZnO and TiO<sub>2</sub> in the Infrared Region of the Spectrum," *Opt. i Spektroskopiya*, Vol. 5, No. 6, pp. 709-711, 1958.
20. Miloslavskii, V. K. and Kovalenko, N. A., "Absorption by Zinc Oxide in the Infrared Region of the Spectrum," *Opt. i Spektroskopiya*, Vol. 5, pp. 614-617, 1958.
21. Collins, R. J. and Kleinman, D. A., "Infrared Reflectivity of Zinc Oxide," *J. Phys. Chem. Solids*, Vol. 11, No. 3-4, pp. 190-194, Oct. 1959.
22. Amberg, C. H. and Seanor, D. H., "An Infrared Study of CO Adsorbed on Surfaces of Zinc Oxide. Influence of Pre-oxidation and Doping," *Proc. 3rd Intern. Congr. Catalysis*, Amsterdam, July 20-25, 1964. National Research Council, Ottawa, Canada, NRC 8029, 1965, AD 618144.
23. Kasai, P. H., "Electron Spin Resonance Studies of Donors and Acceptors in ZnO," *Physiol. Rev.*, Vol. 130, No. 3, pp. 989-995, 1963.
24. Zerlaut, G. A., Gilligan, J. E., and Harada, Y., "Stable White Coatings," Interim Technical Progress Report, IITRI-C6027-16, June 30, 1965.

25. Kokes, R. J., "The Influence of Chemisorption of Oxygen on the Electron Spin Resonance of Zinc Oxide," J. Phys. Chem., Vol. 66, pp. 99-103, 1962.
26. Glemza, R. and Kokes, R. J., "Transient Species in Oxygen Uptake by Zinc Oxide," J. Phys. Chem., Vol. 66, pp. 566-568, 1962.
27. Muller, K. A. and Schneider, J., "Conduction Electron Spin Resonance in Group II-VI, Semiconductors and Phosphors," Phys. Letters, Vol. 4, No. 5, pp. 288-291, May 1963.
28. Baranov, E. V., Kholmogorov, V. E., and Terenin, A. N., "Photoinduced EPR Signals in Zinc Oxide," Dokl. Akad. Nauk SSSR, Vol. 146, No. 1, pp. 125-128, Sept. 1962.
29. Kasai, P. H., "Electronic Spin Resonance Studies of Donors and Acceptors in ZnO," Physiol. Rev., Vol. 130, No. 3, pp. 989-995, May 1963.
30. DeWitt, J. S., "Optical Properties of CdSe and ZnO Single Crystals," School of Engineering, Wright-Patterson AFB, Ohio, SP/PH/65-8, AD 617923, May 1965.
31. Chang, L., "Infrared Coatings Studies - Final Report," Bausch and Lomb, Inc., Rochester, N.Y., Contract DA-44-009-AMC-124 (T), Mod. 1, AD 464854, June 1965.
32. Heiland, G., Mollwo, E., and Stockmann, F., "Electronic Processes in Zinc Oxide," in "Solid State Physics, Advances in Research and Applications," edited by F. Switz and D. Turnbull, Vol. 8, pp. 193-323, 1959.
33. Mollwo, E., "Electrical and Optical Properties of ZnO," in "Photoconductivity Conference," edited by R. G. Breckenridge and B. R. Russell, John Wiley & Sons, 1956.